

3D Continuum Radiative Transfer Images of a Molecular Cloud Core Evolution

J. Steinacker

Max-Planck-Institut für Astronomie, Königstuhl 17, D-69117 Heidelberg

`stein@mpia.de`

and

B. Lang

Max-Planck-Institut für Astronomie, Königstuhl 17, D-69117 Heidelberg

`lang@mpia.de`

and

A. Burkert

Universitäts-Sternwarte München, Scheinerstr.1, D-81679 München

`burkert@usm.uni-muenchen.de`

and

A. Bacmann

Observatoire de Bordeaux, 2 Rue de l'Observatoire, BP 89, 33270 Floirac

`bacmann@obs.u-bordeaux1.fr`

and

Th. Henning

Max-Planck-Institut für Astronomie, Königstuhl 17, D-69117 Heidelberg

`henning@mpia.de`

ABSTRACT

We analyze a 3D Smoothed Particle Hydrodynamics simulation of an evolving and later collapsing pre-stellar core. Using a 3D Continuum Radiative Transfer program, we generate images at 7, 15, 175 μm , and 1.3 mm for different evolutionary times and viewing angles. We discuss the observability of the properties of pre-stellar cores for the different wavelengths. For examples of non-symmetric fragments, it is shown that, misleadingly, the density profiles derived from a 1D analysis of the corresponding images are consistent with 1D core evolution models. We conclude that 1D modeling based on column density interpretation of images does not produce reliable structural information and that multi-dimensional modeling is required.

Subject headings: infrared radiation — ISM: clouds — ISM: dust, extinction — submillimeter — stars: formation

1. Introduction

Molecular cloud cores are thought to be the direct progenitors of stars. However, their initial properties and early evolution are still poorly understood. Current observations therefore aim to find and study these cores in more detail. Density structure, velocity field, and temperature distribution of the gas and dust are key parameters for the physical interpretation of the long lifetimes of these objects. The continuum radiation spectra of deeply embedded sources contain only ambiguous information about the density and temperature distribution of the dust. Column densities can be inferred from the analysis of continuum images in the mm-range (e.g. Ward-Thompson et al. 1994) and the mid-infrared (MIR) (e.g. Bacmann et al. 2000). The emission of molecules within the core contains information about the structure, velocity field (Tafalla et al. 2004, and references therein), and the turbulence (Ossenkopf, Klessen, & Heitsch 2001, and references therein). The currently discussed supporting mechanisms against gravitational collapse are magnetic fields and turbulence. There are a number of simulations treating the full 3D structure of collapsing pre-stellar cores (e.g. Bate, Bonnell, & Bromm 2003; Ballesteros-Paredes, Klessen, & Vázquez-Semadeni 2003; Burkert & Bodenheimer 1993, 2000; Krumholz et al. 2003; Klessen, Heitsch, & Mac Low 2000; Heitsch, Mac Low, & Klessen 2001). In some of these papers, the resulting column density along a line of sight was compared with observationally obtained column densities. The question which structures of the distribution can be seen at which wavelength, however, can only be answered by producing images of the core for given dust properties. In turn, the majority of models that have been applied to observational data are mostly based on spherical symmetry (e.g. André, Ward-Thompson, & Motte 1996). They rely on spherically symmetric models of isolated star formation, which describe core formation, gravitational collapse, and proto-stellar accretion. Commonly, averaged radial density profiles are derived and compared with power-law density distributions (e.g. André, Ward-Thompson, & Motte 1996), or Bonnor-Ebert spheres (e.g. Alves 2004). The major difficulties using 3D models in observations are i) the information loss due to the projection effect, ii) the complex and unique structure of

each individual pre-stellar cores, and iii) the numerical effort of multi-dimensional radiative transfer.

In this letter, we investigate how an evolving cloud core simulated by a 3D Smoothed Particle Hydrodynamics (SPH) code would appear at different wavelengths, which structures are visible, and which density distributions would be inferred using common 1D models. The results from the SPH simulation are described in Sect. 2, along with a discussion of underlying assumptions. We present the images from the 3D Continuum Radiative Transfer (CRT) modeling and discuss the observability of different structures and physical effects. The comparison to density structures obtained from applying 1D models to the images is given in Sect. 3, and the findings are summarized and discussed in Sect. 4.

2. Cloud core evolution model and radiative transfer modeling

2.1. 3D SPH simulation of the evolution of a cloud core

We have calculated the evolution of a cloud core using a three-dimensional SPH code (version described in Bate, Bonnell, & Price 1995), originally developed by Benz, Cameron, Press, & Bowers (1990). The smoothing lengths of particles are variable in time and space, following the constraint that the number of neighbors for each particle has to be approximately constant with $N_{\text{neigh}} = 50$. The SPH equations are integrated using a second-order Runge-Kutta-Fehlberg integrator with individual time steps for each particle (Bate, Bonnell, & Price 1995).

The simulation was initiated with a mass of $M = 3 M_{\odot}$, adopting a spherically symmetric non-rotating homogeneous cloud with a temperature of $T = 10$ K, a diameter of $d = 0.12$ pc (corresponding to a density of 2×10^{-16} kg/m³), and a mean molecular weight $\mu = 2.36 \times 10^{-3}$ kg/mol. This configuration is Jeans unstable. A turbulent velocity field is added only at the beginning of the simulation with a Mach number of $\mathcal{M} = 2$ and following an approximate Kolmogorov law $P(k)d\Omega_k \sim k^{-2}$ for the different modes. The turbulence supports the cloud core against collapse for the first 10^5 yrs. This enables the formation of a pre-stellar core-like structure, self-consistently

as a result of turbulent energy dissipation. A variable equation of state is used: isothermal for densities less than 10^{16} molecules/ m^3 and adiabatic for larger densities.

Deviating from earlier work, the initial conditions are arranged in a way that the core reaches a dynamical equilibrium of density structures and velocity field before it evolves into a runaway collapse. The resulting structure is visualized by iso-density surfaces shown in the left panels of Fig. 1. The top left panel shows the early stage of core formation 5.6×10^4 yrs after the initialization (iso-density of 4×10^{-16} kg/ m^3). Turbulence dominates the structure formation and creates several filamentary low-mass density maxima. The duration of this period before the onset of the collapse and thus the total "age" of the pre-stellar core stage depends on how turbulence is injected initially and its dissipation. In the course of time, the local density enhancements merge. After some additional 8.5×10^4 yrs just at the edge of gravitational instability, a single core has formed (second left panel, 5×10^{-17} kg/ m^3). The kinetic pressure support breaks down due to rapid dissipation of turbulent energy inside the over-dense region and the core starts to collapse ($t = 1.69 \times 10^5$ yrs, third left panel, 5×10^{-17} kg/ m^3). A new single hydrostatic core forms when the gas becomes optically thick and the cooling time exceeds the dynamical time. Later on, the central part of the core is replaced by a sink particle. In the bottom left panel, the structure has flattened substantially, 20% percent of the total mass is already accreted onto the sink particle, and a massive disk has formed through an instability. It contains additional low mass condensations and independently, a second fragment has started to form with a hydrostatic core (5×10^{-17} kg/ m^3). The right panels give the iso-densities for 0.16, 0.5, 1.6, and 5.2×10^{-18} kg/ m^3 for a time of 2.4×10^5 yrs, respectively. With increasing density, the second condensation becomes visible (see also animation at <http://www.mpi-hd.mpg.de/homes/stein/Ani/animcf.htm>).

2.2. 3D CRT modeling of the cores

The SPH density distributions of the gas were discretized on a 3D grid and scaled to dust particle distributions assuming a dust-gas mass ratio of 1/100 and an efficient gas-dust mixing.

The dust number densities were processed with a 3D CRT code (Steinacker et al. 2003, 2002a; Steinacker, Bacmann, & Henning 2002b; Pascucci et al. 2004), producing 640 images of the cloud core at different wavelengths, times, and viewing angles, respectively. The temperatures were calculated from the radiative heating. Heating by compression is irrelevant during the pre-stellar core phase due to the fact that the cooling timescale is much faster than the dynamical timescale. For the illustrative purpose of this letter, we used standard dust opacity data (Drain & Lee 1984) and a standard interstellar radiation field (Black 1994). Some of the images are shown in Fig. 2 for the wavelengths 7, 15, 175, and $1300 \mu m$ (from top to bottom) and evolutionary times of 5.6 and 14.1×10^4 yrs, respectively (left to right). The wavelengths are chosen to cover common observational windows (e.g. ISOCAM, ISOPHOT, IRAM, JCMT, CSO, SPITZER, HERSCHEL). All images are scaled to have maximal contrast. A 10% random background noise representing a mean background variation was added for illustrative purpose only. In the MIR, as expected, the core is visible in absorption and the images reveal much of the outer thin structure especially for the early stages. Detection of the inner, at later stages flattened structure is difficult and requires a careful background analysis. For wavelengths larger than $90 \mu m$, the cold dust can be seen in emission, revealing more of the inner structure at high densities, as the core also starts to get optically thin. This emission is dominating the mm images.

Animations showing the images for all viewing angles at different times of the evolution, as well as visualizations of the 3D density data cube can be found under <http://www.mpi-hd.mpg.de/homes/stein/Ani/animcf.htm>.

3. 1D analysis of the maps

Projection effects are a severe source of misinterpretation for structures seen in absorption or emission, as pointed out already, e.g., by Ballesteros-Paredes & Mac Low (2002). In Fig. 3, we show as an example two structures seen at $7 \mu m$. The upper left panel depicts an elongated filament at an early stage of the evolution (5.6×10^4 yrs), while the upper right panel gives a flattened

structure at a later stage (24.4×10^4 yrs). In the middle panels, the viewing angle was changed until we see the structures as a core-like feature. In the lower panel, they are zoomed and re-binned to an ISOCAM resolution typical for a core at 150 pc distance. We determined the 1D number column density $N(R)$ with the radius in the plane of the sky R by azimuthally averaging over annuli. As the absorption patterns have elliptical shape, we have used elliptical annuli. The resulting number column density was inverted to a 1D number density distribution $n(r)$ with the radius r using recursive integration. In Fig. 4, we show the results for the early stage-filament in the main panel and for the later stage-disk in the inset. The range of profiles $n(r)$ which have been transformed from $N(R)$ -profiles along individual directions is given by the solid thin lines and the direction-averaged profile is plotted as solid thick line. The dashed line indicates the slope of a density distribution following a r^{-2} -power-law as it was derived from 1D core evolution models (Shu 1977). Although these absorption maxima are slightly less extended than commonly observed cores, the 1D model seems to provide a reasonable description of the derived distributions. It could be inferred from this fit that the underlying density structure has an elliptical shape with a profile that - transformed to a spherical distribution - is in agreement with 1D core evolution models. To compare with the true underlying 3D density distribution, we calculated the number density n for a grid of equally-sized cells from the SPH density distribution. For each cell, we determined the distance to the center of the "core"-distribution defining a point in the $n(r)$ -diagram. This point distribution was rebinned to a grayscale image for better clarity, where black refers to maximum number of cells per bin. The advantage of this representation is that a 1D core with radial power law appears as a line in the $n(r)$ -diagram with a gradient representing the powerlaw index.

The true density distributions overlayed as grayscale-image are far from being lines as the filament is not 1D spherically symmetric. The agreement with the 1D evolution models would tend to validate static core formation models, although the core formation mechanism modeled here is highly dynamical. This is in agreement with the findings of Ballesteros-Paredes, Klessen,

& Vázquez-Semadeni (2003). We also modelled the flattened structure at a later stage. The radial profile within the disk will be visible in our grayscale-representation of $n(r)$ as a line with the slope of the power-law exponent, and indeed the inlet in Fig. 4 shows a pronounced branch of the disk-like structure. If the core-flattening is confirmed by an independent source of information, the column density profiles (and the resulting density profiles) can be used to determine the radial profile of the disk-like structure.

4. Conclusions

We have presented 3D simulations assuming that initially low mass condensations pass through a stage of turbulence dominated condensation where they accumulate mass and merge together to form extended pre-stellar core like objects. The typical density structures in the cores are non-spherical throughout their evolution. The asymmetry is driven by the turbulent motion and causes complex structures from the very beginning. This complexity is partially seen in images that have been calculated from the densities obtained in the cloud core simulation. However, projection effects can lead to a severe misinterpretation of images. We showed that a 1D analysis of the vicinity of the density maxima would suggest a density profiles in agreement with 1D core collapse models. The underlying density structure, however, is intrinsically three-dimensional and deviates strongly from the obtained 1D model distribution.

As the column density also enters the optical thin emission in the mm-range (aside from the Planck function), we expect the same projection ambiguities to occur when interpreting mm-maps of dense molecular cloud regions. This aspect will be discussed in a forth-coming paper.

We conclude that 1D modeling based on column density interpretation of images does not produce reliable structural information. For flattened structures appearing in later stages of the core evolution, a 2D modeling might be applicable, but for the general case, multi-dimensional continuum and line radiative transfer modeling is required to derive consistent density and temperature distributions of the gas and dust in pre-stellar cores.

REFERENCES

- Alves, J. 2004, *Ap&SS*, 289, 259
- André, P., Ward-Thompson, D., Motte, F. 1996, *A&A*, 314, 625
- Bacmann, A., André, P., Puget, J.-L., Abergel, A., Bontemps, S., Ward-Thompson, D. 2000, *A&A*, 361, 555
- Ballesteros-Paredes, J. & Mac Low, M. 2002, *ApJ*, 570, 734
- Ballesteros-Paredes, J., Klessen, R. S., & Vázquez-Semadeni, E. 2003, *ApJ*, 592, 188
- Bate, M. R., Bonnell, I. A., & Bromm, V. 2003, *MNRAS*, 339, 577
- Bate, M. R., Bonnell, I. A., & Price, N. M. 1995, *MNRAS*, 277, 362
- Black, J.H. 1994, *ASP Conference Series*, 58, 355
- Benz, W., Cameron, A. G. W., Press, W. H., & Bowers, R. L. 1990, *ApJ*, 348, 647
- Burkert, A. & Bodenheimer, P. 2000, *ApJ*, 543, 822
- Burkert, A. & Bodenheimer, P. 1993, *MNRAS*, 264, 798
- Draine, B.T., Lee, H.M. 1984, *ApJ*, 285, 89
- Heitsch, F., Mac Low, M., & Klessen, R. S. 2001, *ApJ*, 547, 280
- Klessen, R. S., Heitsch, F., & Mac Low, M. 2000, *ApJ*, 535, 887
- Krumholz, M. R., Fisher, R. T., Klein, R. I., & McKee, C. F. 2003, *Revista Mexicana de Astronomia y Astrofisica Conference Series*, 15, 138
- Ossenkopf, V., Klessen, R.S., & Heitsch, F. 2001, *A&A*, 379, 1005
- Pascucci, I., Wolf, S., Steinacker, J., Dullemond, C. P., Henning, T., Niccolini, G., Woitke, P., & Lopez, B. 2004, *A&A*, 417, 793
- Shu, F.H. 1977, *ApJ*, 214, 488
- Steinacker, J., Henning, Th., Bacmann, A., & Semenov, D. 2003, *A&A*, 401, 405
- Steinacker, J., Hackert, R., Steinacker, A., & Bacmann, A. 2002a, *JQSRT*, 73, 557
- Steinacker, J., Bacmann, A., & Henning, Th. 2002b, *JQSRT*, 75, 765
- Tafalla, M., Myers, P.C., Caselli, P., Walmsley, C.M. 2004, *A&A*, 416, 191
- Ward-Thompson, D., Scott, P.F., Hills, R.E., André, P. 1994, *MNRAS*, 268, 276



Fig. 1.— Iso-density surfaces of the averaged SPH density distributions of a cloud core fragment. The left panel shows densities of 40, 5, 5, and $5 \times 10^{-17} \text{ kg/m}^3$ at the times 5.6, 14.1, 16.9, and 27.2×10^4 yrs after the start of simulation, respectively. The right panel gives iso-density surfaces at the time 24.4×10^4 yrs and densities of 0.16, 0.5, 1.6, and $5.2 \times 10^{-18} \text{ kg/m}^3$, respectively.

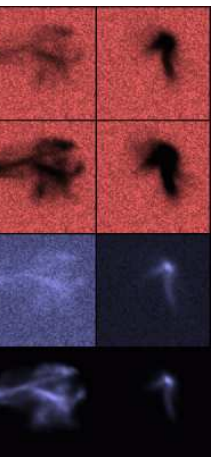


Fig. 2.— Images of the cloud core fragment at the wavelengths 7, 15, 175, and 1300 μm (left columns from top to bottom), and at the times 5.6 and 14.1×10^4 yrs after start of simulation (left to right), respectively.

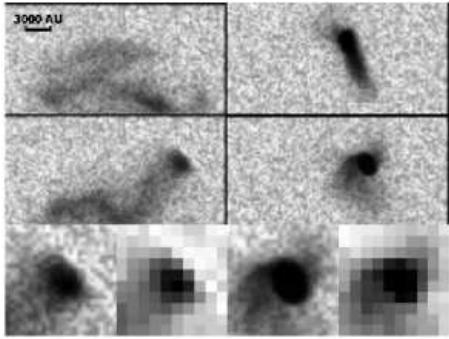


Fig. 3.— Examples of features in $7\ \mu\text{m}$ images mimicking dense cores. The top panels show structures which look like a core when choosing an appropriate viewing angle (middle panels). The lower panels zoom into the core-like structures and switch to ISOCAM resolution.

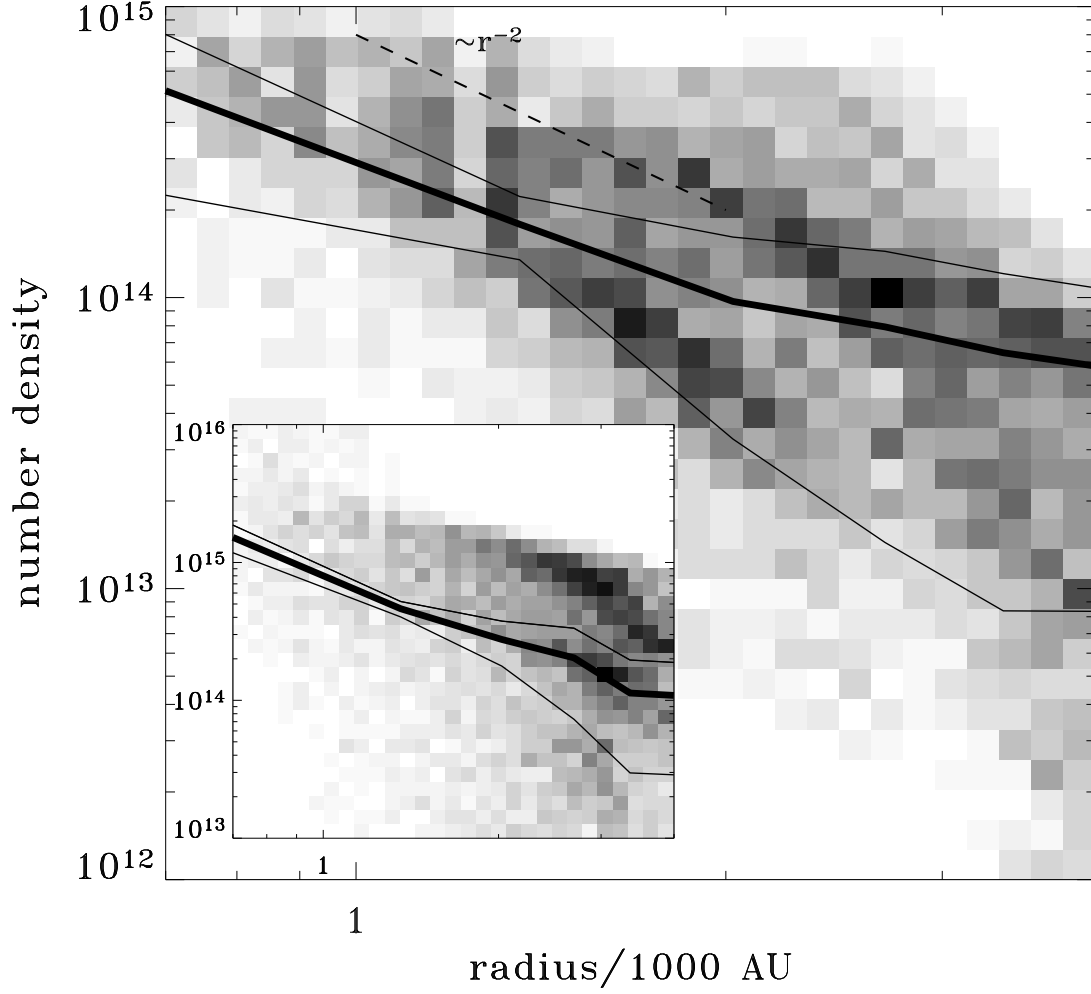


Fig. 4.— 1D density profiles $n(r)$ obtained from the $7\ \mu\text{m}$ -image by azimuthally integrating the column density around the absorption maximum along elliptical tracks. The thin solid lines mark the range of profiles for individual directions, and the direction-averaged profile is represented by the thick solid line. The dashed line indicates an r^{-2} -dependency. The true 3D density distribution n_{SPH} was discretized on a cell grid, and transformed to a point distribution in the $n(r)$ -plane. The number of points is shown as gray-scale image where black means maximum number of grids with a certain density. The main picture corresponds to an elongated filament from the early stage, and the inset to a flattened structure from a later stage of the core evolution, respectively.